



Determining the Critical Region and Reusability of CNG All-Steel Cylinders in Collision

M. Yazdani Ariatapeh^{1*}, M. Mashayekhi², S. Ziaei Rad²

¹*School of Mechanical Engineering, Isfahan University of Technology, Tehran, Iran*

²*Faculty of Mechanical Engineering, Isfahan University of Technology, Tehran, Iran*

Abstract: In this paper damage mechanics approach has been applied to investigate the effect of impact and damage caused by that in under pressure CNG All-steel cylinders by using ABAQUS\Explicit. The CSA standard in CNG cylinders is used as a damage detection criterion and cylinders ability to reuse. Simulation of cylinder failures caused by collision has been done by using Johnson-Cook damage model. Accomplished simulations are carried out in different impact directions, and effect of cylinder internal pressure and collision velocity are analyzed. These investigations for different cases show that the maximum damage created in case of vertical impact and by changing direction from vertical to horizontal resultant damage will be decreased. The results show that in collision process the cylinder's rear wall and the front hemisphere of cylinder have more damaged and are the critical areas in the horizontal and vertical collisions, respectively. For a specific impact direction in lower cylinder internal pressure and higher collision velocity damage will be more. The resulted diagrams indicate that damaged area of the cylinders predominately are under compression and endure large plastic deformation.

Keywords: *All-steel CNG cylinder, Damage Mechanics, collision, fracture, reusability.*

1. Introduction

High cost and risk of empirical tests make the use of numerical methods inevitable. From economical view, natural gas is frugal fuel by low cost and with abundant resources, on the other hand this combustion pollution are lower than other common fossil fuels such as gasoline and diesel. A major issue of natural gas fuel using in cars, is the storing problem. CNG cylinders in cars with compressed natural gas fuel are used for gas storage at high pressure. These cylinders is divided into four categories according to the manufacturer's material that including: all-metal, metal liner hoop wrapped, metal liner fully wrapped and all-composite. All-steel cylinders with 91.7 percent usage are the most common type of cylinders and history of these cylinders goes back to 1974. There are three known methods to produce this type of cylinders so that their difference is in the raw material. Safety is one of the important issues in design and manufacturing of such cylinders. All-metal cylinders are using more well-known

technology with respect to the other types of cylinders and therefore have more capability to safe performance. According to the importance of safety and decrease concern of gaslight car's passengers, because of incident due to CNG cylinders impact with barriers especially in car accidents, it is necessary to investigate cylinder impact conditions before use. Despite this, almost no studies have been reported specially on impact phenomenon of the CNG cylinders but the similar studies have noted as the following works.

In 1991, Becker et al. [1] to ensure that the reactor pressure vessel/neutron shield tank assembly could be shipped safely without undue risk to the public or the environment, the reactor pressure vessel/neutron shield tank assembly was certified by the U.S. Department of Energy as a type B package. A safety analysis report for packaging was prepared in accordance with U.S. Department of Energy requirements to provide the technical basis for the U.S. Department of Energy certification. The reactor pressure vessel/neutron shield tank

* - E-mail: (m.yazdaniariatape@me.iut.ac.ir)



package is a monolithic structure of lightweight concrete and steel. To substantiate multidimensional inelastic analyses, a series of drop tests was conducted on several benchmark models from various heights. Technical evaluation and correlation of the test data were performed in conjunction with the structural analysis and assessment of the package. This research provides a comprehensive discussion on the benchmark drop models and specific drop tests and also addresses the results obtained from comparing technical data with analytical data. The purpose of the benchmark tests was to demonstrate that the results of the structural analyses of the package are a reasonable representation of its real structural behavior.

In 1994, Rosenberg et al. [2] a series of experiments was conducted on high pressure vessels made of stainless steel in order to determine the critical pressures for catastrophic failure under projectile impact. By using gas dynamics calculations based on an ideal gas equation of state expanding isothermally through the hole in the pressurized cylinder and adiabatic expansion of a non-ideal gas they found that, they shall assume a constant pressure within the vessel throughout the whole process. In 2006, Nagel and Thambiratnam [3] The aim of this paper is to compare the energy absorption response of straight and tapered thin-walled rectangular tubes under oblique impact loading, for variations in the load angle, impact velocity and tube dimensions. All computer modelings in this study were conducted using the nonlinear finite element (FE) code ABAQUS/Explicit version 6.3. It is found that the mean load and energy absorption decrease significantly as the angle of applied load increases. Nevertheless, tapering a rectangular tube enhances its energy absorption capacity under oblique loading. The outcome of the study is design information for the use of straight and tapered thin-walled rectangular tubes as energy absorbers in applications where oblique impact loading is expected. According to various studies cylinder internal pressure, projectile kinematic energy and characteristics of cylinder are effective factors in damage

affected by the impact on under pressure cylinders.

2. Problem Analysis Method

The ductile fracture criteria among the various fracture approaches of metals such as: Stress intensity factor and J- integral, cohesive element method and the Gurson model, due to uncoupled equations reduced the solution time. Compared with the other model, these fracture criteria can be relatively easily calibrated and implemented in FE codes, and thus have been widely used in industrial practices [4]. This type of fracture criteria could be implemented in ABAQUS/Explicit and used, as regard this criteria by less coefficients and more accurate calibration are appropriate for using on impact problem. All the damage models based on this criterion are assumed to be uncoupled with the material constitutive model in that the condition for fracture is checked at each step outside the loop of stress and strain calculation. When an accumulated damage indicator reaches a critical value, an element suddenly fails and completely loses its load-carrying capability.

Among damage model based on ductile fracture criteria the Johnson–Cook model formulated in the space of the stress triaxiality and the equivalent plastic strain to fracture are capable of predicting the realistic fracture patterns and at the same time the correct residual velocities, thus this model is suitable for prediction of fracture caused by impact problem [5]. Johnson and Cook [6] developed a constitutive model to describe material properties under dynamic loading. The von Mises yield surface with the associated flow rule is used in this material model. Its isotropic hardening law includes effects of strain rates and temperature rise. In companion with their material constitutive equation, Johnson and Cook [7] proposed a fracture criterion for dynamic loading problems. Similarly to the material constitutive model, the fracture strain was assumed to be a function of the stress triaxiality, strain rates, and temperature in an uncoupled form, defined by:



$$\bar{\sigma} = \left[A + B \varepsilon_{pl}^n \right] \left[1 + C \ln \left(\frac{\dot{\varepsilon}_{pl}}{\dot{\varepsilon}_0} \right) \right] \left[1 - \left(\frac{T - T_0}{T_m - T_0} \right)^q \right] \quad (1)$$

$$\varepsilon_f = \left[D_1 + D_2 \exp \left(D_3 \frac{\sigma_h}{\bar{\sigma}} \right) \right] \left[1 + D_4 \ln \left(\frac{\dot{\varepsilon}_{pl}}{\dot{\varepsilon}_0} \right) \right] \left[1 + D_5 \frac{T - T_0}{T_m - T_0} \right] \quad (2)$$

where $\bar{\sigma}$ is the von Mises stress; σ_h hydrostatic pressure; ε_{pl} is the effective plastic strain; $\dot{\varepsilon}_{pl}$ and $\dot{\varepsilon}_0$ are the current and reference strain rates; T_m and T_0 are the melting and room temperature, respectively; A , B , n , C , q and D_1 , ..., D_5 are ten material constants which need to be calibrated from experiments. This model accounts for isotropic strain hardening, strain rate hardening and temperature softening in the uncoupled form.

The first term in the brackets in the right hand side of Eq. (2) has the same form as proposed by Hancock and Mackenzie [8], and represents fracture characteristics of a specimen under quasi-static loading conditions at room temperature. Since an exponential function was employed in the first term, Johnson and Cook implied that the fracture locus could be represented by one continuous curve in the entire range and the fracture strain decreases with the increasing stress triaxiality. In a general case, the stress triaxiality is not a constant but varies during a loading process. Johnson and Cook [7] assumed that damage accumulates in a linear way, i.e.

$$D = \int_0^{\varepsilon_{pl}} \frac{1}{\varepsilon_f} d\varepsilon_{pl} \quad (3)$$

An element fails when D reaches unity, i.e. $D_{cr} = 1.0$. The stress triaxiality, defined as the ratio of the hydrostatic pressure to the von Mises stress, is commonly introduced in the literature to represent the stress state mentioned in Eq. (2). Note that the hydrostatic pressure is the first invariants of the stress tensor and the von Mises stress is the square root of the second invariant. Both invariants are independent of a coordinate system, and thus suitable for large plastic deformation. Impact problems involve large plastic deformation, high strain rates, and

elevated temperature. Due to high strain rates, heat generated by a large portion of plastic energy would not have sufficient time to escape to surrounding materials, which leads to temperature rise. Both strain rates and temperature clearly have an effect on fracture characteristics of a specimen. According to the features that were counted on for Johnson–Cook's model and existing in ABAQUS/Explicit, it is used in the present paper.

3. Problem Analysis

In this section discusses about the modeling and analysis of the CNG cylinders on collision and the result of the simulations are explained.

3.1 Preliminary Cylinder Simulation

60-lit cylinder manufactured by Faber company in Italy by the height of the cylindrical section 668 mm, the external diameter of 318 mm and inner diameter of 301.8 mm for cylindrical and two end hemisphere is used in simulations according to figure 1. The cylinder is made of 4340 alloy steel, JC material and damage model constants for this steel extracted according table 1.

All computer modelings in this study were conducted using the ABAQUS/Explicit version 6.10. For collision cases horizontal and vertical directions are considered. The CSA standard for CNG cylinder are used to targeted meshing, evaluation of impact damage and ability to reuse of the cylinder after collision. This association lists general guidelines, CNG cylinder damage is classified in three levels. The levels are as follows [9]:

Level 1 - any scratch, gouge, or abrasion with a damage depth of less than or equal to .010 inch (0.25 mm). First level damage is acceptable and does not need to be repaired.

Level 2 - any scratch, gouge, or abrasion with a damage depth of 0.011 to 0.050 inch (0.27 to 1.27 mm). Second level damage requires rework (either in the field or by the manufacturer), a more thorough evaluation, or

destruction of the cylinder depending on severity.

Level 3 - any scratch, gouge, or abrasion with a damage depth greater than .050 inch (1.27 mm). Third level damage is severe enough that the cylinder cannot be repaired and must be destroyed. All fire, and chemical damage is Level three, if it does not wash off.

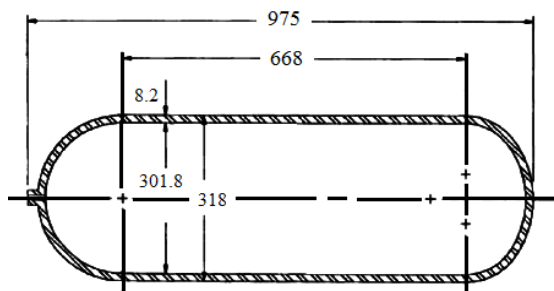


Fig. 1: Scheme of the Faber all-steel cylinder in term of mm [10].

Thus fine meshes are used to depth of 1.27 mm from outer surface of cylinder wall and also the areas that are directly under the impact have finer meshes where fracture was expected to occur, while relatively coarse meshes were used in the other part of the cylinder. This action will reduce computational costs. 8-node, linear brick elements with reduced integration (C3D8R) were used. Failed elements are removed to illustrate the formation and growth of cracks. The kinematic contact constraint was prescribed at the impact interface, which allows the projectile to elastically rebound from the rigid wall at the end of the impact process. The friction coefficient between the front surface of the cylinder and the rigid walls is assumed to be 0.1. Process time in the simulations 20 ms is considered that the damage during this period reached to the constant value. For all state of impact failed area in critical damaged regions, damage and other parameters diagrams, that affecting in JC damage model, at the point of these areas were drawn and studied.

3.2 Cylinder Simulation on Collision

In this section CNG Cylinder has been analyzed in vertical and horizontal collision to investigate the effect of collision directions on

the amount of damage in the cylinder. Due to the symmetry existing in the problem, the One-half cylinder model is considered and at the cut edges of the cylinder, the symmetry boundary condition is applied.

According to figures 2 and 3, in the created FE models for simulation of the cylinder collision two cube-shaped rigid surfaces are considered in which first surface is as the cylinder support in the accident and the other as the colliding object.

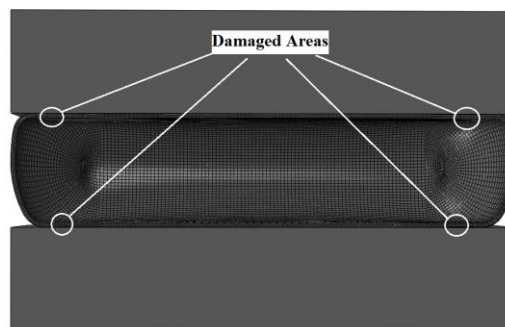


Fig. 2: Deformed model of the cylinder after horizontal collision



Fig. 3: Deformed model of the cylinder after vertical collision.

To investigate the effect of internal pressure of the cylinder and the object's collision velocity on the amount of damage to the cylinder, for each simulated collision direction, 200 bars pressure (cylinder working pressure) and the 50 bars pressure has uniformly applied to the inner surface of the cylinder and the speed of 180 km/h which is the critical velocity and speed of 120 km/h which is the maximum velocity limit on highways have been applied to the reference point of the rigid object. Comparing the amount of damage on both sides of the cylinder shows that in horizontal collision the behind wall of the cylinder and in vertical collision the lens in front of cylinder have been more damaged than other areas and are considered as critical areas.

By removing damaged elements in the affected areas, in Figures 4 to 6, it is observed that for horizontal collision in working pressure and different velocities, depth of damage in the cylinder wall compared with the values expressed in CSA Standard, the cylinder can be used if it is repaired again, but under the pressure of 50 bars and in velocity of 180 km/h depth of damage exceeded the amount of acceptable damage and the cylinder is considered out of work and must be changed. In all states of vertical collision, depth of damage in the cylinder wall exceeded the acceptable amount of damage and the cylinder is considered out of work. Under the pressure of 50 bars and in the same conditions the level of indentation depth is greater than working pressure which shows that under less internal pressure the amount of damage is more.

Figures 7 and 8 show that the damage in all cases has grown rapidly and after a short time it becomes constant and in vertical direction compared to horizontal direction the amount of damage accumulation for the same conditions was about twice; consequently, the number of omitted elements is more. Also, it can be concluded that in less pressure and more velocity the amount of accumulated damage for each specific direction is more.

Comparing the history of equivalent plastic strain between critical points of collision on Figures 9 and 10, shows that this quantity follows same damage trend too. Here, also in the vertical direction, less pressure and higher colliding velocity creates more plastic strain.

The history of the stress triaxiality for critical area in various directions of collision at figures 11 and 12 show that these areas in a great part of collision process under the stress triaxiality less than -0.5 which indicates that critical zone is predominantly under compression. After beginning the collision process, further drop has occurred in the critical region of the graph of vertical collision which indicates that the higher compression is due to bending in this direction.

Figure 13 shows the damage rate for collision in working pressure along 180 km/h for a point in the critical area in vertical and horizontal direction and, for the outer wall of the cylinder

to a depth of 1.27 mm (maximum depth of damage) has five and ten nodes. The closeness of results to each other indicates that the obtained response does not depend on the meshing.

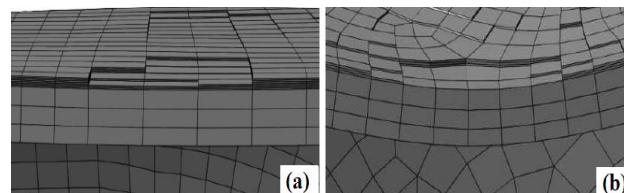


Fig. 4: Damaged critical area in the collision for working pressure and the velocity of 120 km/h: (a) the horizontal direction, (b) the vertical direction.

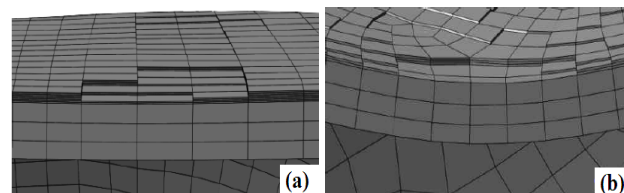


Fig. 5: Damaged critical area in the collision for working pressure and the velocity of 180 km/h: (a) the horizontal direction, (b) the vertical direction.

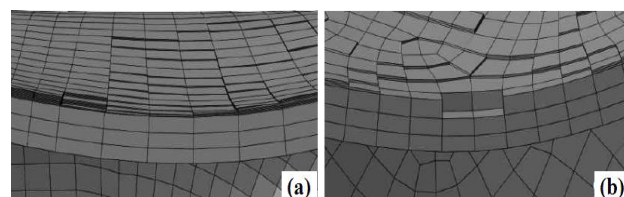


Fig. 6: Damaged critical area in the collision for the pressure of 50 bars and the velocity of 180 km/h: (a) the horizontal direction, (b) the vertical direction.

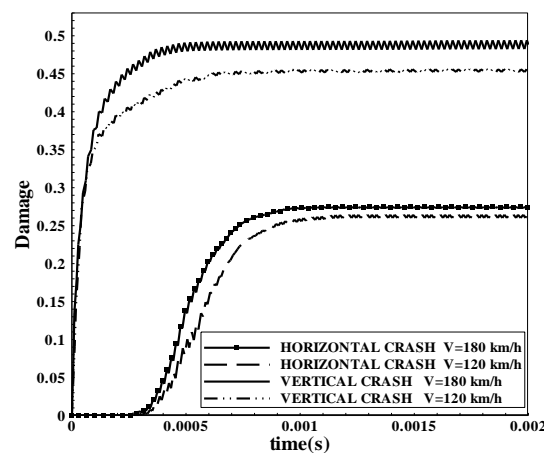


Fig. 7: Damage growth at a point of the critical damaged area in the working pressure.

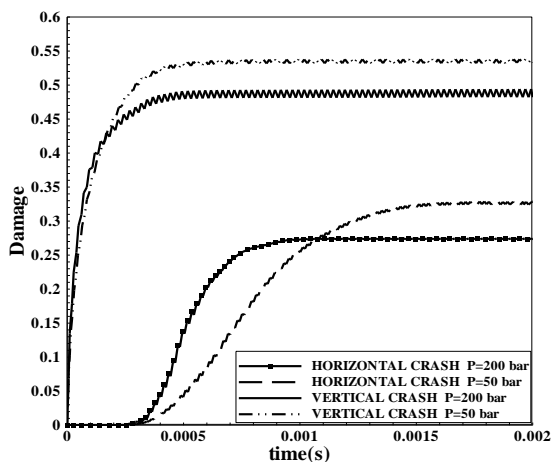


Fig. 8: Damage growth at a point of the critical damaged area in the collision velocity of 180 km/h.

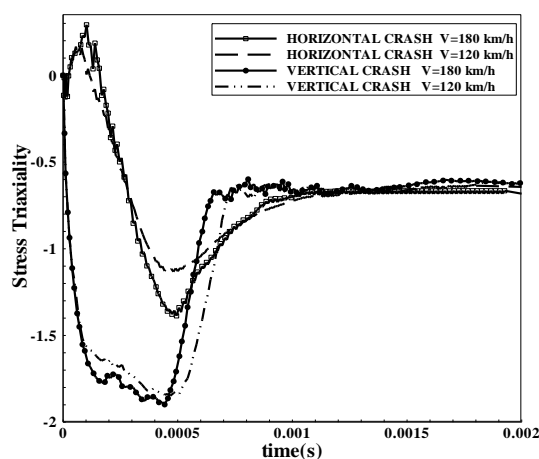


Fig. 11: History of the stress triaxiality at a point of the critical damaged area in the working pressure.

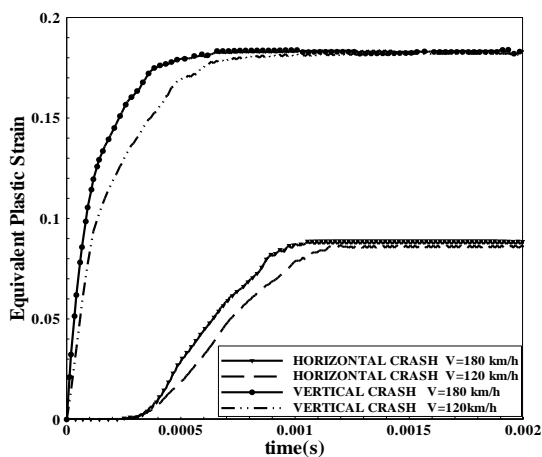


Fig. 9: History of the equivalent plastic strain at a point of the critical damaged area in the working pressure.

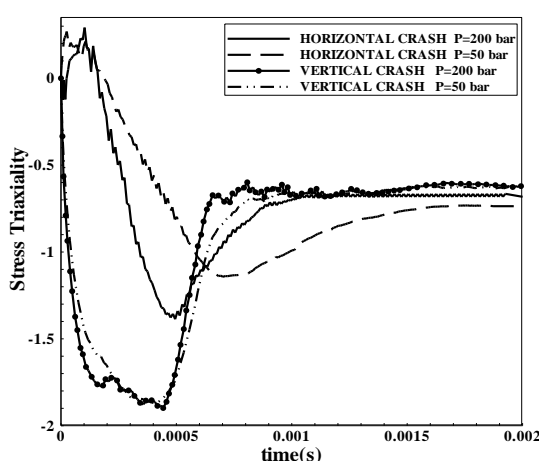


Fig. 12: History of the stress triaxiality at a point of the critical damaged area in the collision velocity of 180 km/h.

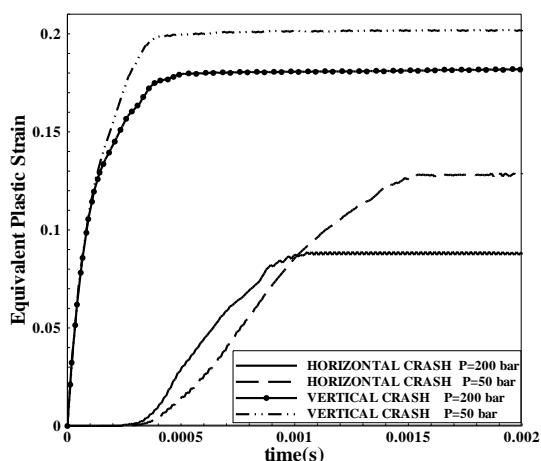


Fig. 10: History of the equivalent plastic strain at a point of the critical damaged area in the collision velocity of 180 km/h.

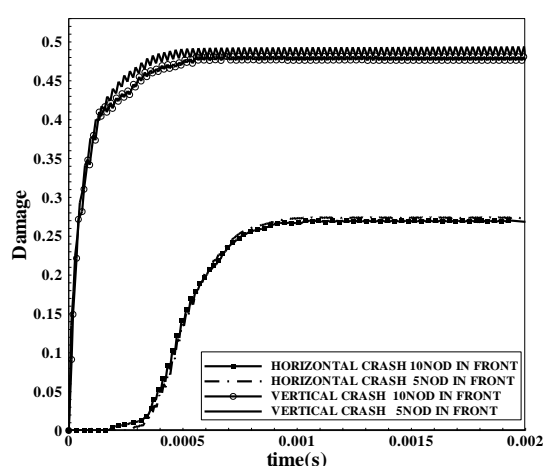


Fig. 13: Damage growth in the collision for different directions in working pressure and the velocity of 180 km/h for the 5 and 10 nodes in outer wall of the cylinder.



Table 1

Material and damage model constant for 4340 alloy steel [7].

E (GPa)	ν	ρ (kg/m ³)	T_m (K)	T_0 (K)	C_v (J/kg.K)
200	0.29	7830	1793	293	477
α (K ⁻¹)	A (MPa)	B (MPa)	n	C	m
0.000032	792	510	0.26	0.014	1.03
$\dot{\epsilon}_0$ (s ⁻¹)	D ₁	D ₂	D ₃	D ₄	D ₅
1	0.05	3.44	-2.12	0.002	0.061

4. Conclusion

This paper has examined the effect of direction and collision velocity and internal pressure on the damage in All-steel CNG cylinders by using damage mechanic approach. Investigating the diagrams shows that the maximum quantity of damage caused in the vertical direction and by changing the impact direction from vertical to horizontal damage value will be decreased. Also by eliminating failed elements and comparing damage depth caused by collision with CSA standard, it is observed that in most cases of vertical accident, cylinders have been damaged and lose its ability to use, while in horizontal impact cases cylinder is intact or can be reused after repairing. The results show that in collision process the cylinder's rear wall and the front lense of cylinder have more damaged and are the critical areas in the horizontal and vertical collisions, respectively. For a specific impact direction in lower internal pressure and higher collision velocity damage will be more. Also, the damaged areas are predominantly under compression and have suffered a high plastic strain. The low difference between the results by various meshes shows that this solution does not depend on the mesh size. Therefore, this damage model is insensitive to meshing in the various impact cases.

Acknowledgements

I would like to express my deep gratitude to Dr. Mohammad Mashayekhi for his guidance, support, and encouragement during my two years at IUT. Thanks are due to Professor Saeed Ziaei Rad for taking time to teach me finite Elements and for his valuable advice and patience during my M.Sc. degree course at IUT. I gratefully acknowledge my parents and my family for their understanding and support.

References

- [1] Becker, D. L., Burgess, D. M. and Lindquist, M. R. "Drop Testing Conducted to Benchmark the Shipping port Reactor Pressure Vessel Package Safety Analysis", Nuclear Engineering and Design, 130, 1991, pp. 133-145.
- [2] Rosenberg, Z., Mironi, J., Cohen, A. and Levy, P. "On the Catastrophic Failure of High-Pressure Vessels by Projectile Impact", Int. J. Impact Engng, 15, 1994, pp. 827-831.
- [3] Nagel, G. M. and Thambiratnam, D. P. "Dynamic Simulation and Energy Absorption of Tapered Thin Walled Tubes under Oblique Impact Loading", Int. J. Impact Engng, 32, 2006, pp. 1595-1620.
- [4] Teng, X. "High Velocity Impact Fracture", PhD thesis, Massachusetts Institute of Technology, 2004.
- [5] Teng, X. and Wierzbicki, T. "Evaluation of Six Fracture Models in High Velocity Perforation", Engng Fract Mech, 73, 2006, pp. 1653-1678.
- [6] Johnson, G. R. and Cook, W. H. "A Constitutive Model and Data for Metals Subjected to Large Strains, High Strain Rates and High Temperatures", in: Proceedings of the seventh international



- symposium on ballistics. Hague, Netherlands, 1983, pp. 541–47.
- [7] Johnson, G. R. and Cook, W. H. "Fracture Characteristics of Three Metals Subjected to Various Strains, Strain Rates, Temperatures and Pressures", *Engng Fract Mech*, 21(1), 1985, pp. 31–48.
- [8] Hancock, J. W. and Mackenzie, A. C. "On the Mechanisms of Ductile Failure in High Strength Steels Subjected to Multi-axial Stress-States", *Journal of the Mechanics and Physics of Solids*, 24, 1976, pp. 147–169.
- [9] CSA America Inc. "CNG Fuel System Inspector Study Guide", National Energy Technology Laboratory, U.S. Department of Energy, DE-FC26-05NT42608, 2008.
- [10] T Ribarits, S. G., "Assessment of Inspection Criteria and Techniques for Recertification of Natural Gas Vehicle (NGV) Storage Cylinders", M.Sc. thesis, Mechanical Engineering Department, University of British Columbia, 1983.